Thrombosis Research 177 (2019) 23–32

Contents lists available at ScienceDirect

Thrombosis Research

journal homepage: www.elsevier.com/locate/thromres

Full Length Article

Exosomes of bone-marrow stromal cells inhibit cardiomyocyte apoptosis under ischemic and hypoxic conditions via miR-486-5p targeting the PTEN/PI3K/AKT signaling pathway

Xiang-Hua Sun[a,b], Xu Wang[c], You Zhang[d], Jie Hui[a,*]

[a] Department of Cardiology, The First Affiliated Hospital of Soochow University, Suzhou 215006, PR China
[b] Department of Cardiology, Shaoyang Central Hospital, Shaoyang 422000, PR China
[c] Department of Cardiovascular Surgery, The First Affiliated Hospital of Soochow University, Suzhou 215006, PR China
[d] Department of Cardiology, The Second Affiliated Hospital of Soochow University, Suzhou 215004, PR China

ARTICLE INFO

Keywords:
BMSC
Exosome
MiR-486-5p
PTEN/PI3K/AKT
Apoptosis
Myocardial ischemia-reperfusion injury

ABSTRACT

Background: Myocardial ischemia–reperfusion injury (MIRI) is a major obstacle in the treatment of ischemic heart disease. Recent studies have shown that exosomes—small membrane vesicles secreted by most cell types—could have a protective effect on the ischemic myocardium. In this study we explored the effect of exosomes derived from bone-marrow stromal cells (BMSC-exo) on cardiomyocyte apoptosis and MIRI.

Methods: Exosomes were purified from culture media using the ExoQuick kit and observed using transmission electron microscopy. Cell viability was assessed by 3-(4,5-dimethyl-2-thiazolyl)-2,5-diphenyl-2-H-tetrazolium bromide (MTT) assay. Cell apoptosis was analyzed by flow cytometry using the Annexin-V/PI stain. The expression levels of microRNA (miRNA), messenger RNA (mRNA) and PTEN/PI3K/AKT-pathway-related proteins were detected by qRT-PCR and western blot, respectively. Myocardial ischemia was simulated by incubating H9C2 cells in a hypoxia/reoxygenation (H/R) conditioned rat MIRI model.

Results: BMSC-exo induced the proliferation of H9C2 cells and rescued H9C2 cells from apoptosis in the H/R model, indicating that BMSC-exo has a protective effect on cardiomyocyte injury caused by H/R. Using transgenic H9C2 cells, we found that miR-486-5p in BMSC-exo suppressed the H/R-triggered apoptosis of H9C2 cells. In addition, BMSC-exo repressed the expression of PTEN in H9C2 cells via miR-486-5p, and subsequently activated the PI3K/AKT pathway in vitro. Moreover, the myocardial injury caused by ischemia/reperfusion was repaired by BMSC-exo which activates the PI3K/AKT pathway via miR-486-5p *in vivo*.

Conclusion: Our results suggested that exosomes from BMSCs have a protective effect on myocardium ischemic injury. MiR-486-5p carried by BMSC-exo plays a pivotal role in the regulatory process by suppressing PTEN expression, activating the PI3K/AKT signaling pathway, and subsequently inhibiting the apoptosis of injured cardiomyocytes.

1. Introduction

Ischemic heart disease (IHD) is a serious threat to human health and is one of the leading causes of mortality and disability worldwide. The basic physiological process of IHD is myocardial ischemia. Current treatments of IHD—including drugs, percutaneous coronary intervention and coronary artery bypass grafting—work effectively to alleviate the ischemia-induced myocardial injury and necrosis through recovery of myocardium blood perfusion [1]. However, there is a good chance that restoring blood reperfusion after myocardial ischemia could result in further damage to myocardial cells; this is known as myocardial ischemia–reperfusion injury (MIRI) [2,3]. Research has shown that several processes could be involved in MIRI, including increased production of oxygen free radicals, inflammation, calcium overload, and the opening of mitochondrial permeability transition pores (MPTPs) during the blood perfusion [4]. So far, there is no accessible clinical treatment method which effectively avoids MIRI, which leads to severe limitations of the therapeutic efficacy of current IHD treatments.

In a previous study, cardiomyocyte apoptosis was found to be a typical phenomenon involved in the process of MIRI [5]. Moreover, the

* Corresponding author at: Department of Cardiology, The First Affiliated Hospital of Soochow University, No. 188, Shizi Street, Soochow 215006, Jiangsu Province, PR China.
E-mail address: huijie92@163.com (J. Hui).

https://doi.org/10.1016/j.thromres.2019.02.002
Received 3 September 2018; Received in revised form 14 January 2019; Accepted 1 February 2019
Available online 02 February 2019

apoptosis of the injured cardiomyocytes is not only triggered by myocardial ischemia, it is also induced by myocardial reperfusion which recovers the blood supply [6,7]. Thus, the study of suppression of cardiomyocyte apoptosis could be a valid approach to finding potential treatments which could mitigate MIRI injury.

Exosomes are small (30–100 nm) membrane vesicles secreted by most cell types [8]. Exosomes are generated from the inward budding of multivesicular endosomes (MVE). When MVEs fuse with the cell membrane, exosomes (containing proteins, mRNAs and miRNAs from the cytoplasm) are released [9]. Binding with specific ligands, exosomes recognize and enter target cells by endocytosis or by fusing with the target cell membrane [10,11]. In this way, exosomes serve as mediators of distant cell-to-cell signaling, and play regulatory roles in several process such as immune regulation [12], apoptosis, tissue regeneration, angiogenesis [13–15], and myocardial remodeling [16,17]. In addition, exosomes from specific origins—such as cardiac progenitor cells [18], induced pluripotent stem cells [19] and mesenchymal stem cells [17]—have been reported to have protective effects on MIRI. Nevertheless, the mechanism by which exosomes protect cardiomyocytes from MIRI remains unclear.

A previous report has claimed that miRNAs in exosomes could serve as key factors in the regulatory process of exosomes in the ischemic myocardium [20]. A class of small endogenous RNAs, miRNAs are important regulators in eukaryocytes by targeting mRNAs with complementary sequences and inhibiting protein translation [21]. For the exosomes derived from mesenchymal stem cells (MSC-exo), it was reported that miR-146a in MSC-exo inhibited the apoptosis of cardiomyocytes and protected the injured myocardium [22]. Furthermore, Feng et al. reported that miR-22 in MSC-exo suppressed the raising of methyl CpG binding protein-2 (Mecp2) expression and inhibited the apoptosis of cardiomyocyte [23]. These studies showed the protective effect of MSC-exo on MIRI, which was mediated by the miRNAs carried within the exosomes. Bone-marrow-derived mesenchymal stem cells (BMSCs) also showed a potential therapeutic effect on myocardium ischemia. The transplantation of BMSCs could improve cardiac function and the structural remodeling following myocardial infarction by promoting the expression of functional miRNAs or inhibiting the expression of aberrant miRNAs in a paracrine manner [24]. Previous studies showed that miR-486-5p—an miRNA targeting the PTEN and Akt pathway—is enriched in exosomes from BMSCs (BMSC-exo) [25,26]. Recent evidence suggests that miR-486-5p has a protective effect on cardiomyocytes and ischemia/reperfusion (I/R) injury. In cardiomyocytes, miR-486-5p inhibits the apoptosis triggered by hydrogen peroxide [27] and alleviates the hypoxia-induced damage, including cell viability, migration, invasion and apoptosis [28]. Moreover, miR-486-5p carried by exosomes derived from human endothelial colony-forming cells reduces kidney I/R injury [26]. The regulatory effect of miR-486-5p from BMSC-exo on cardiomyocytes and MIRI remains unclear.

In this study, we focused on the effect of BMSC-exo on cardiomyocyte apoptosis and MIRI. We found that exosomes from BMSCs have a significant protective effect on cardiomyocyte apoptosis and MIRI, in which miR-486-5p played an important role. MiR-486-5p from BMSC-exo suppressed PTEN expression in cardiomyocytes, and then activated the PI3K/Akt signaling pathway, inhibiting cardiomyocyte apoptosis and ischemic injury of the myocardium.

2. Methods

2.1. Cell culture

Rat bone-marrow mesenchymal stem cells were isolated using Sprague Dawley rats (specific-pathogen-free) (Vital River, Beijing, China). All animal studies were approved by the local committee for Animal Care and Ethics of The First Affiliated Hospital of Soochow University. Rats were dipped in 75% ethanol for 5–10 min after sacrifice. Hind limbs were clipped and peeled, then knee joints were cut. The femur and tibia were severed from the hip and ankle, with ligaments, and muscles and excess tissue were removed. Bones were opened both ends to expose the marrow shaft. After the remove of femoral epiphyses, the medulla was flushed with Dulbecco's modified Eagle's medium (DMEM) (Gibco; Carlsbad, CA, USA) supplemented with 10% fetal bovine serum (FBS) (Hyclone; Logan, UT, USA) and 1% penicillin–streptomycin (Gibco; Carlsbad, CA, USA) on ice. Impurities were filtered out and cells were collected by centrifuge. Cells were resuspended, plated in dishes and cultured in 5% CO_2 at 37 °C. Non-adherent cells were removed, and the culture medium was changed after 48 h. Cells were trypsinized using 0.25% trypsin and then subcultured at a ratio of 1:3 when cells were confluent. BMSCs at P3 to P8 were used in this study.

H9C2 cells (Cell Bank of Chinese Academy of Sciences; Beijing, China) were cultured in DMEM supplemented with 10% FBS, 100 U/mL penicillin and 100 μg/mL streptomycin at 37 °C with 5% CO_2.

2.2. Exosome isolation and NanoSight tracking analysis

BMSCs were cultured in medium without serum for 48 h. Culture medium was collected and further concentrated by centrifugation for 30 min at 2000 ×*g* to remove cells and debris, followed by filtration through a 0.22-μm filter to thoroughly remove the large extracellular vesicles. Exosomes were further purified using the Total Exosome Isolation (from cell culture media) kit (Thermo, USA) following the manufacturer's protocol. In brief, samples were mixed with 0.5 volumes of the Total Exosome Isolation reagent by vortex and incubated overnight at 4 °C. Exosomes were then harvested by centrifugation for 60 min at 10,000 ×*g* at 4 °C. The pellet was resuspended in 1× phosphate-buffered saline (PBS). The particle size distribution and quantification of exosomes isolated were characterized by Nano S90 (Zetasizer Nano S90). The data were processed by Nano S90 analytical software.

2.3. Electron microscopy

Resuspended exosomes were dropped on the copper mesh-grids coated with Formvar/carbon film and incubated for 1 min. Then excess liquid was removed, and the grids were contrasted with 2% phosphotungstic acid (PTA). Grids containing exosomes were observed by transmission electron microscopy (Jem 1400, Jeol, Japan) at 80 kV.

2.4. Western blot

Cells were harvested, washed with 1 × PBS and lysed with lysis buffer (Sigma-Aldrich; St Louis, MO, USA). The cell lysate was collected, and the protein concentration was determined using the bicinchoninic acid protein assay (Vigorous). Proteins were resolved with SDS-PAGE and transferred to nitrocellulose membranes. Membranes were blocked in 2.5% skim milk for 1 h, incubated overnight with the primary antibody to CD9, CD63, ALIX, TSG101, Bax, c-caspase-3, Bcl-2, PTEN, PI3K-p110a, p-AKT and AKT (Cell Signaling; Danvers, MA, USA, 1:1000 dilution) and glyceraldehyde 3-phosphate dehydrogenase (GAPDH) (Cell Signaling; Danvers, MA, USA, 1:4000 dilution) at 4 °C. After washing three times with PBS, the membranes were incubated with the second antibody (ZSGB-Bio; Beijing, China, 1:5000 dilution) for 1 h. The bands of proteins were detected using a chemiluminescence detection system (CWBIO; Beijing, China).

2.5. Cell viability assay

The cell viability was assessed using the 3-(4,5-dimethyl-2-thiazolyl)-2,5-diphenyl-2-H-tetrazolium bromide (MTT) assay. BMSCs were plated into 96-well culture plates at an initial density of 600 cells per well. After treatment, 20 μL MTT reagent (5 mg/mL; Sigma-Aldrich; St

Louis, MO, USA) was added to each well. After 4 h incubation at 37 °C, the supernatant was removed, and the formazan crystals were dissolved with 150 μL dimethylsulfoxide (DMSO, Sigma-Aldrich; St Louis, MO, USA). The absorbance of each well was assessed at 490 nm using the Microplate System. Experiments were conducted in triplicate.

2.6. H/R treatment of cardiomyocytes

To simulate an I/R injury model in vitro, H9C2 cells were induced by H/R treatment. H9C2 cells were first cultured in DMEM medium (glucose- and serum-free) and exposed to a humidified incubation chamber flushed with 95% N_2 and 5% CO_2 for hypoxic incubation at 37 °C. After 16 h, the cells were transferred to a reoxygenation medium (high-glucose DMEM medium containing 10% FBS) and cultured in 5% CO_2 at 37 °C for 3 h.

2.7. RNA isolation and quantitative real-time polymerase chain reaction (qRT-PCR) assay

Total RNA and exosome RNA were isolated using TRIzol reagent (Sigma-Aldrich; St Louis, MO, USA), and then reverse transcribed into cDNA using TransScript reverse transcriptase (Transgene; Beijing, China) with random primer or miRNA reverse transcription primer. Primers of mRNA for qRT-PCR were designed using Primer-BLAST (https://www.ncbi.nlm.nih.gov/tools/primer-blast). qRT-PCR was performed at 95 °C for 2 min, followed by 40 cycles at 95 °C for 15 s, 60 °C for 10 s and 68 °C for 25 s. The relative expression levels of target genes were determined using the formula $2^{-\triangle\triangle Ct}$. Primers were ordered from Ribobio (Guangzhou, China). The primer sequences were as follows. MiR-486-5p-F: 5′-GCGTCCTGTACTGAGCTGC-3′, miR-486-5p-R: 5′-CGGCCCAGTGTTCAGACTAC-3′; PTEN-F: 5′-ATTCCCAGTCAGAG GCGCTA-3′, PTEN-R: 5′-TCACCTTTAGCTGGCAGACC-3′; GAPDH-F: 5′-ACAGCAACAGGGTGGTGGAC-3′, GAPDH-R: 5′-TTTGAGGGTGCAGC GAACTT-3′; U6-F: 5′-CTCGCTTCGGCAGCACA-3′, U6-R: 5′-AACGCTTC ACGAATTTGCGT-3′. GAPDH and U6 were used as the internal controls for mRNA and miRNA identification, respectively. Samples lacking cDNA were used as negative controls.

2.8. Lentiviral construction and infection

Lentivirus vectors pHBLV (Genechem; Shanghai, China) were used for the construction of miRNA overexpression/suppression vectors. The pre-miRNA of miR-468-5p and anti-miR-486-5p were synthesized from Genechem (Shanghai, China). The oligos were dissolved using annealing buffer, denatured in a 98 °C water bath for 15 min, then cooled to room temperature. The annealed fragments were subcloned into lentivirus vectors and amplified. The packaging and production of lentiviruses were performed according to the manufacturer's protocol. The miRNA overexpression/suppression vectors and lentivirus packaged plasmid were co-transfected into HEK293T cells using Lipofectamine 3000 (Invitrogen, ThermoFisher; Shanghai, China). H9C2 cells were cultured in six-well plates at a density of 1×10^5 per well and infected at 37 °C. Fresh medium was added 12 h after transfection; 24 h after infection, fresh medium supplemented with puromycin was changed for further selection. Cells were harvested 10 days after puromycin selection for identification and further study.

2.9. Luciferase reporter assay

The 3′-untranslated region (3′-UTR) of PTEN was amplified by high-fidelity PCR and inserted into the psiCHECK-2 luciferase reporter vector (Promega; Madison, Wisconsin, USA). H9C2 cells were plated in 24-well plates 24 h before transfection. H9C2 cells were transfected with 200 ng of the 3′-UTR luciferase reporters vector (Ambion; Austin, TX, USA) using lipofectamine 3000 reagent according to the manufacturer's instructions. Medium was removed 6 h after transfection, and exosomes were added in fresh medium. Cells were lysed 24 h later, and the luciferase activity was assessed with a microplate system using luciferase assay kits (Promega, Beijing, China). The expression of luciferase was presented as the ratio of *Renilla* luciferase gene to firefly luciferase gene.

2.10. Myocardial I/R model

Sprague Dawley male rats were anesthetized by intraperitoneal injection of sodium pentobarbital (50 mg/kg; Sigma-Aldrich; St Louis, MO, USA). An incision was made in the left thorax, the heart was exteriorized, and a slipknot (6–0 silk) was made around the left anterior descending coronary artery (LAD). After 30 min, the slipknot was removed, and reperfusion was allowed for 3 h. At the beginning of the reperfusion, rats were injected with 200 μL PBS containing 400 μg exosomes/control (n = 7/group) via the tail vein. After 3 h, the left anterior descending coronary artery was re-ligated and 2 mL Evans blue dye (1.0%) was infused into the carotid artery catheter to distinguish ischemic zones from non-ischemic zones. The heart was then excised, washed using physiological saline, and stored at −80 °C. All animal experimental procedures were conducted following the Guide for the Care and Use of Laboratory Animals.

2.11. 2,3,5-Triphenyltetrazolium chloride (TTC) stain

The evaluation of myocardial infarction was performed using 2% 2,3,5-triphenyltetrazolium chloride (TTC) stain. Frozen hearts were sliced into sections 1 mm thick; the sections were stained with 2% (w/v) TTC diluted in phosphate buffer (88 mM Na_2HPO_4 and 1.8 mM NaH_2PO_4) at 37 °C for 20 min in the dark. Then sections were fixed using 10% formalin solution and photographed to calculate the myocardial infarction area.

2.12. Cell apoptosis assay

Following treatment, the apoptosis rate of H9C2 cells was analyzed by flow cytometry with the Annexin V–FITC apoptosis detection kit (Sigma-Aldrich; St Louis, MO, USA), according to the manufacturer's instructions. In brief, cells were trypsinized, washed with chilled PBS, and resuspended in binding buffer; 5 μL FITC-labeled Annexin V reagent were added to 190 μL cell suspension. After gentle mixing, 5 μL propidium iodide (PI) solution was added to the cell suspension. The cells were incubated in the dark for 15 min at room temperature and then analyzed using flow cytometry (BD Biosciences).

2.13. Statistical analysis

Data are showed as means ± SDs of at least three repeated experiments. One-way ANOVA followed by the Tukey post-hoc test was conducted across comparison among multiple comparisons, and unpaired Student *t*-test was used for two-group comparisons; $p < 0.05$ was considered statistically significant. All statistical analyses were conducted using GraphPad Prism 5.0 (GraphPad Software, Inc., La Jolla, CA, USA).

3. Results

3.1. Isolation and identification of exosomes from BMSCs

Exosomes were isolated from BMSC culture supernatant and observed using transmission electron microscopy (TEM). The exosomes purified from BMSC culture supernatant (BMSC-exo) were evenly scattered across the view as rounded particles, which is characteristic morphology for exosomes (Fig. 1A). The size distribution of exosomes was analyzed by the Nano Measurer. The peak BMSC-exo diameter was around 50 nm (Fig. 1B). To further ensure the quality of the exosomes in our isolation, we used western blot to assess the presence of several

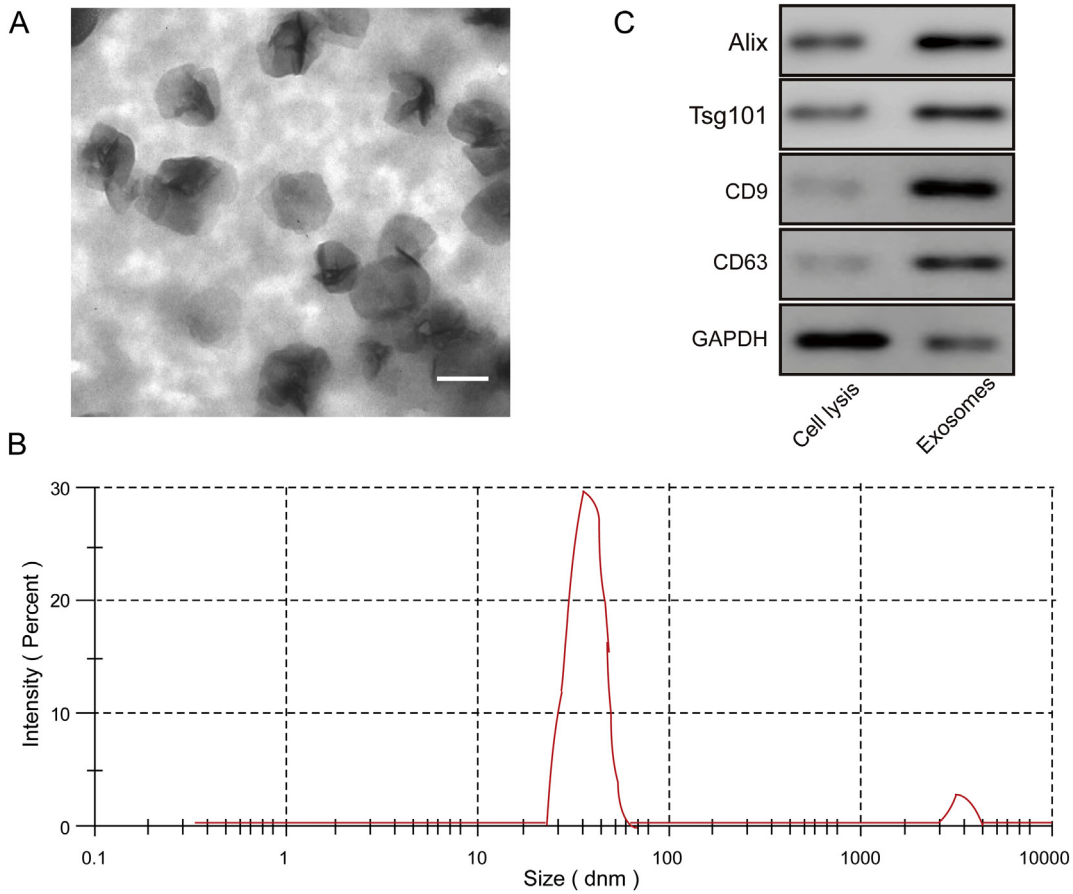

Fig. 1. The identification of exosomes derived from bone-marrow stromal cells (BMSCs). (A) Representative image of exosomes isolated from BMSC culture supernatant (BMSC-exo) using transmission electron microscopy. Scale bar: 50 nm. (B) The size distribution of exosomes was analyzed by the Nano Measurer. The diameter of exosomes ranges mainly from 35 nm to 100 nm. (C) Western blot analysis of protein levels of CD9, CD63, Alix and Tsg101 in cell lysis and BMSC-exo. Glyceraldehyde 3-phosphate dehydrogenase (GAPDH) was used as internal control.

common exosome/vesicle markers, including CD9, CD63, Alix and Tsg101 (Fig. 1C). CD9, CD63, ALIX and TSG101 are highly expressed in isolated exosomes but lowly or rarely expressed in lysed cells. The morphological observation and the assessment of representative markers of exosomes demonstrated that the isolated exosomes qualified for further investigation.

3.2. BMSC-exo significantly inhibited cardiomyocyte apoptosis induced by H/R

To investigate the effect of BMSC-exo on cardiac ischemic injury, we treated cardiomyocytes with BMSC-exo and then assessed the apoptosis status induced by H/R. H9C2 cells were cultured with media containing BMSC-exo at different concentrations from 0 to 800 μg/mL. The proliferation rates of H9C2 were then assessed after 48 h. The MTT experiment showed that treatment of BMSC-exo induced proliferation of H9C2 cells in a dose-dependent manner. Furthermore, at concentrations ≥ 400 μg/mL, BMSC-exo significantly enhanced the proliferation rate of H9C2 cells (Fig. 2A). We then assessed the effect of BMSC-exo on the apoptosis of cardiomyocytes triggered by H/R. After 16 h of hypoxia and 3 h of reoxygenation, H9C2 cells were incubated in a medium with/without BMSC-exo (400 μg/mL) for 24 h. Analysis by flow cytometry showed that H/R induced cell apoptosis in H9C2 cells significantly (from about 9% to 34%), while the treatment of BMSC-exo in the process of reoxygenation repressed the apoptosis of H9C2 cells in H/R conditions (from about 34% to 21%), showing that BMSC-exo partially rescued cells from H/R injury (Fig. 2B, C). Furthermore, in the assessment of expression levels of proteins related to cardiomyocyte apoptosis, it was shown that H/R treatment induced the expression of c-caspase-3 and Bax but repressed the expression of Bcl-2. However, the involvement of BMSC-exo reversed the variable expression of c-caspase-3, Bax and Bcl-2 under H/R conditions (Fig. 2D). Thus, the data showed that BMSC-exo partially rescued the apoptosis of H9C2 cells induced by H/R conditions, indicating that BMSC-exo could have a protective effect against cardiomyocyte injury caused by H/R.

3.3. MiR-486-5p in BMSC-exo inhibited cardiomyocyte apoptosis induced by H/R

First, we assessed the expression level of miR-486-5p in H9C2 cells in H/R conditions using qRT-PCR and observed significant down-regulation of miR-486-5p in H/R conditions (Fig. 3A). To further clarify the effect of miR-486-5p in BMSC-exo on cardiomyocytes, we overexpressed miR-486-5p and anti-miR-486-5p (the inhibitor of miR-486-5p) in BMSC cells. The overexpression vectors of miR-486-5p and anti-miR-486-5p were conducted into BMSC cells. Vectors of scrambled miRNA (miR-NC and anti-miR-NC) were used as negative controls. The exosomes were purified, and the expression level of miR-486-5p was detected by qRT-PCR. The level of miR-486-5p in BMSC-exo was up-regulated about 10-fold in the exosomes derived from miR-486-5p-overexpressed BMSCs and was down-regulated about 50% in the exosomes derived from miR-486-5p-inhibited BMSCs (Fig. 3B). The effect of miR-486-5p differentially expressed BMSC-exo (*exo*-miR-486-5p and exo-anti-miR-486-5p) on the viability of H9C2 cells was further investigated. MTT assay showed that *exo*-miR-486-5p was better able to induce the proliferation of H9C2 cells than BMSC-exo, while the exo-

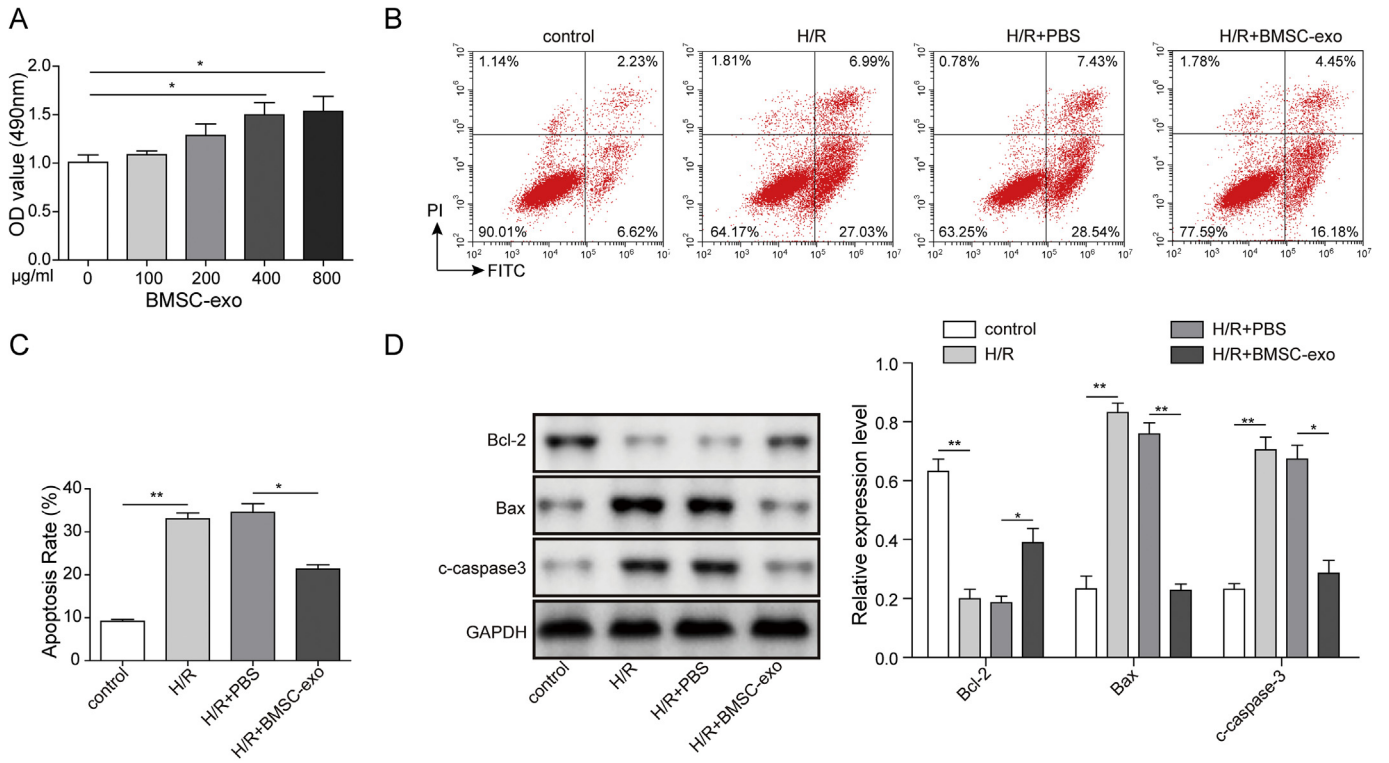

Fig. 2. Exosomes derived from bone-marrow stromal cells (BMSC-exo) suppressed the apoptosis of cardiomyocytes induced by hypoxia/reoxygenation (H/R). (A) Plots of the proliferation rate of H9C2 cells treated with BMSC-exo at concentrations 0, 100, 200, 400 or 800 μg/mL. Cells were harvested after 48 h (n = 3). (B, C) Representative images (B) and plots of flow cytometry analysis (C) of H9C2 cells' apoptosis rate with or without BMSC-exo treatment (400 μg/mL) in the H/R model. H9C2 cells were hypoxic for 16 h, then reoxygenated for 3 h. Cells were harvested 24 h after reoxygenation (n = 3). (D) Western blot analysis of protein levels of Bcl-2, Bax and c-caspase-3 in H9C2 cells treated with BMSC-exo in the H/R model. H9C2 cells were hypoxic for 16 h, then reoxygenated. Cells were harvested 24 h after reoxygenation. Glyceraldehyde 3-phosphate dehydrogenase (GAPDH) was used as internal control. $*p < 0.05$, $**p < 0.01$; n = 3.

anti-miR-486-5p suppressed viability of H9C2 cells (Fig. 3C). In the apoptosis assay, compared with BMSC-exo and exo-miR-NC (exosomes from miR-NC-overexpressed BMSCs), exo-miR-486-5p significantly repressed the apoptosis of H9C2 cells triggered by H/R, whereas exo-anti-miR-486-5p treatment resulted in a significantly higher apoptosis rate (Fig. 3D, E). The expression of Bcl-2 and Bax proteins were evaluated by western blot. Exo-miR-486-5p inhibited the expression of Bax and promoted the level of Bcl-2 in H/R-treated H9C2 cells. For the exo-anti-miR-486-5p, the regulatory effect on Bcl-2 and Bax was the opposite of that of the overexpression group (Fig. 3F). As a result, the level of miR-486-5p in BMSC-exo was positively correlated with the suppression effect of BMSC-exo on H/R-triggered cell apoptosis of H9C2, suggesting that miR-486-5p plays a pivotal role in the process of BMSC-exo inhibiting cardiomyocyte apoptosis triggered by H/R.

3.4. BMSC-exo could target PTEN and activate the PI3K/AKT signaling pathway in cardiomyocytes via miR-486-5p

Previous studies have reported that PTEN could be a potential target of miR-486-5p. However, the interaction between miR-486-5p and PTEN remains unclear in H9C2 cells. To further investigate the mechanism of miR-486-5p regulating the apoptosis of H/R-treated cardiomyocytes, we constructed reporting vectors expressing luciferase fused with the 3′-UTR of the PTEN gene containing wild-type or mutated target sequences of miR-486-5p to evaluate the recognition of PTEN 3′-UTR by miR-486-5p. The complementary schema between the seed region of miR-486-5p and 3′-UTR of PTEN are showed in Fig. 4A. Reporter plasmids were transfected into H9C2 cells; the cells were then treated with BMSC-exo/*exo*-miR-486-5p/exo-anti-miR-486-5p/exo-NC for 24 h. The dual-luciferase reporting system showed that BMSC-exo, exo-NC and exo-miR-486-5p inhibited the activity of the luciferase-fused wild-type 3′-UTR region of PTEN. Besides, *exo*-miR-486-5p acted as a better inhibitor of the reporter's activity compared with BMSC-exo or BMSC-NC. On the other hand, compared with *exo*-NC, exo-anti-miR-486-5p increased the luciferase activity (Fig. 4B). Exosomes from all origins have no regulatory effect on luciferase fused with a mutated 3′-UTR region of PTEN (Fig. 4B). In addition, using qRT-PCR assay, we assessed the expression of PTEN in H9C2 cells treated with BMSC-exo/*exo*-miR-486-5p/*exo*-anti-miR-486-5p/exo-NC and got consistent results with the dual-luciferase assay (Fig. 4C). Given that PTEN/PI3K/AKT constitutes an important pathway that regulates cell apoptosis [29], we also assessed the levels of PI3K and AKT in H/R-treated cardiomyocytes. Compared with BMSC-exo, exo-miR-486-5p had a stronger effect on reducing the protein level of PTEN and inducing the protein levels of PI3K-p110a and p-AKT, while the exo-anti-miR-486-5p showed the opposite effect on the protein levels of PTEN, PI3K-p110a and p-AKT (Fig. 4D). To further clarify the involvement of the PTEN/PI3K/AKT signaling pathway in the process of BMSC-exo's regulation in cardiomyocytes, we co-treated H9C2 cells under H/R conditions with *exo*-miR-486-5p and an inhibitor of PI3K, LY294002. We found that the induction of PI3K and p-AKT triggered by exo-miR-486-5p was blocked significantly (Fig. 4D). The results suggested that in cardiomyocytes BMSC-exo repressed the expression of PTEN via miR-486-5p and subsequently activated the PI3K/AKT signaling pathway.

3.5. BMSC-exo protected cardiomyocytes from I/R injury via miR-486-5p/PTEN/PI3K/AKT pathway in vivo

To further confirm the results from the cell experiments in vitro, we modeled myocardial ischemia reperfusion in rats by ligating the left anterior descending branch of the coronary artery; the effect of BMSC-exo and miR-486-5p on I/R-injured myocardium was verified.

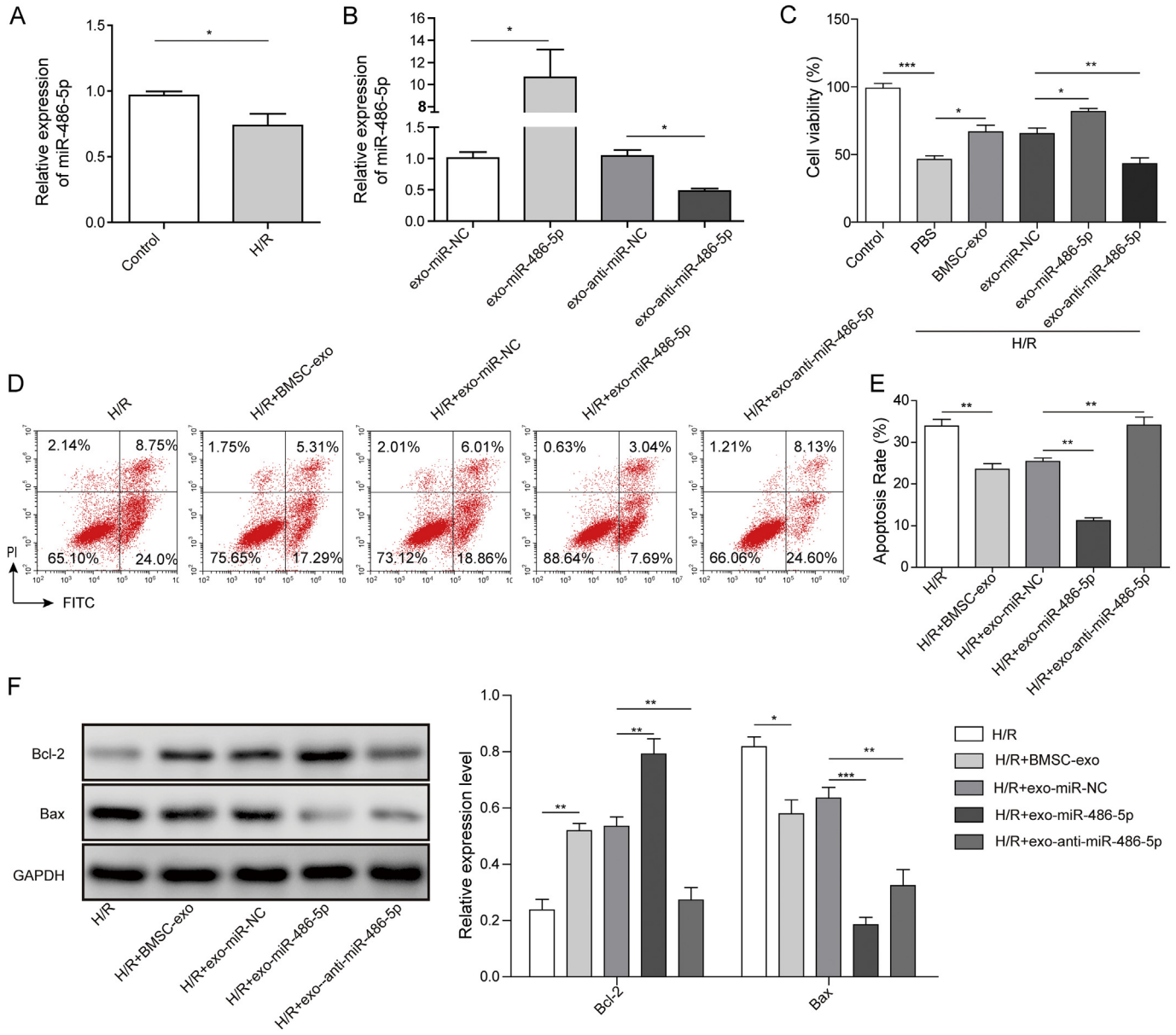

Fig. 3. MiR-486-5p from exosomes derived from bone-marrow stromal cells (BMSC-exo) inhibited the apoptosis of cardiomyocytes in the hypoxia/reoxygenation (H/R) model. (A) The relative expressions of miR-486-5p in H9C2 cells in the H/R model was detected by qRT-PCR (n = 3). (B) Plots of relative expressions of miR-486-5p in exosomes from BMSC cells that overexpressed with miR-486-5p (*exo*-miR-486-5p), anti-miR-486-5p (anti-exo-miR-486-5p) and scrambled miRNA (exo-miR-NC), respectively (n = 3). (C) Plots of cell viability ratio of H9C2 cells treated with BMSC-exo, exo-miR-486-5p, anti-exo-miR-486-5p and exo-miR-NC in the H/R model (n = 3). (D, E) Representative images (D) and plots (E) of flow cytometry analysis of H9C2 cells' apoptosis rate with treatment of exosomes from different origins in the H/R model (n = 3). (F) Western blot analysis of protein levels of Bcl-2 and Bax in H9C2 cells treated with exosomes from different origins in the H/R model (n = 3). Glyceraldehyde 3-phosphate dehydrogenase (GAPDH) was used as internal control. $*p < 0.05$, $**p < 0.01$, $***p < 0.001$.

Exosomes from different origins were injected via the tail vein with the reperfusion, and the myocardial infarction was stained using TTC. Results showed that the injection of BMSC-exo and *exo*-miR-486-5p with the reperfusion decreased the area of myocardial infarction. Furthermore, the overexpression of miR-486-5p enhanced the protective effect of BMSC-exo. However, exo-anti-miR-486-5p treatment resulted in a larger area of myocardial infarction compared with BMSC-exo treatment (Fig. 5A). In addition, BMSC-exo activated the PI3K/AKT pathway and induced cell apoptosis in I/R. Western blot showed that in the I/R process BMSC-exo treatment significantly suppressed the expression of PTEN, Bax and c-caspase-3 while inducing the expression of PI3K-p110a, p-AKT, and Bcl-2. Compared with BMSC-exo treatment, the overexpression of miR-486-5p enhanced the regulatory effect of BMSC-exo on each factor related with the PTEN/PI3K/AKT pathway and cell apoptosis, while the inhibition of miR-486-5p suppressed the effect (Fig. 5B–H). The data suggested that BMSC-exo reduced MIRI *in vivo* via miR-486-5p, which suppressed PTEN, activated the PI3K/AKT pathway, and inhibited the apoptosis of cardiomyocytes.

4. Discussion

Myocardial ischemia is the underlying mechanism of ischemic heart disease, which is a leading cause of mortality in the world. As a main form of myocardial injury, cardiomyocyte apoptosis in myocardial ischemia has been extensively investigated [30–33]. It is important to find treatments which effectively suppress cardiomyocyte apoptosis and protect the myocardium from ischemic injury or MIRI. Several studies have reported that exosomes from different origins could regulate the

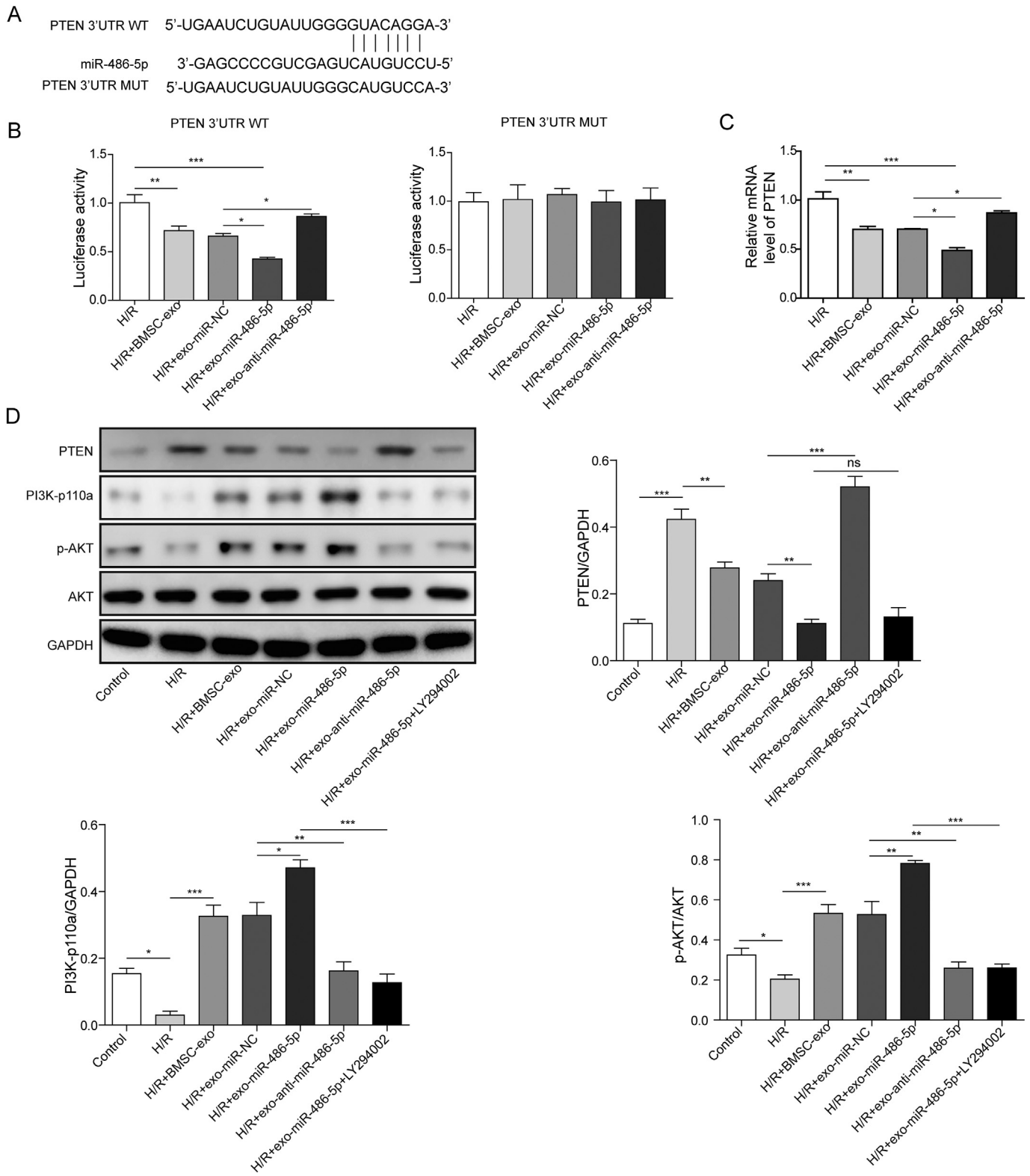

Fig. 4. MiR-486-5p from exosomes derived from bone-marrow stromal cells (BMSC-exo) suppressed the PTEN/PI3K/AKT signaling pathway. (A) Schematic representation of PTEN 3′-UTR containing the predicted conserved target site of miR-486-5p and the mutant type3′-UTR of PTEN inserted in the luciferase reporter assay. (B) H9C2 cells were transfected with wild-type 3′-UTR of PTEN (PTEN 3′ UTR WT) or mutant type 3′-UTR of PTEN (PTEN 3′ UTR MUT) reporter vector and cultured with BMSC-exo, *exo*-miR-NC, exo-miR-486-5p or exo-anti-miR-486-5p, respectively. The relative luciferase levels of reporter were assessed using a luciferase reporter assay system. The results are plotted as relative expression compared to phosphate-buffered saline (PBS) treatment (n = 3). (C) PTEN relative expression of H9C2 cells treated with exosomes from different origins were detected by qRT-PCR (n = 3). (D) Western blot analysis of protein levels of PTEN, PI3K-p110a, p-AKT and AKT in H9C2 cells treated with BMSC-exo/exo-miR-NC/exo-miR-486-5p/exo-anti-miR-486-5p/exo-miR-486-5p + LY294002 in the hypoxia/reoxygenation (H/R) model. LY294002 was added in medium at the beginning of hypoxic incubation at a concentration at 30 μM (n = 3). Cells were harvested 24 h after reoxygenation. Glyceraldehyde 3-phosphate dehydrogenase (GAPDH) was used as internal control. *$p < 0.05$, **$p < 0.01$, ***$p < 0.001$.

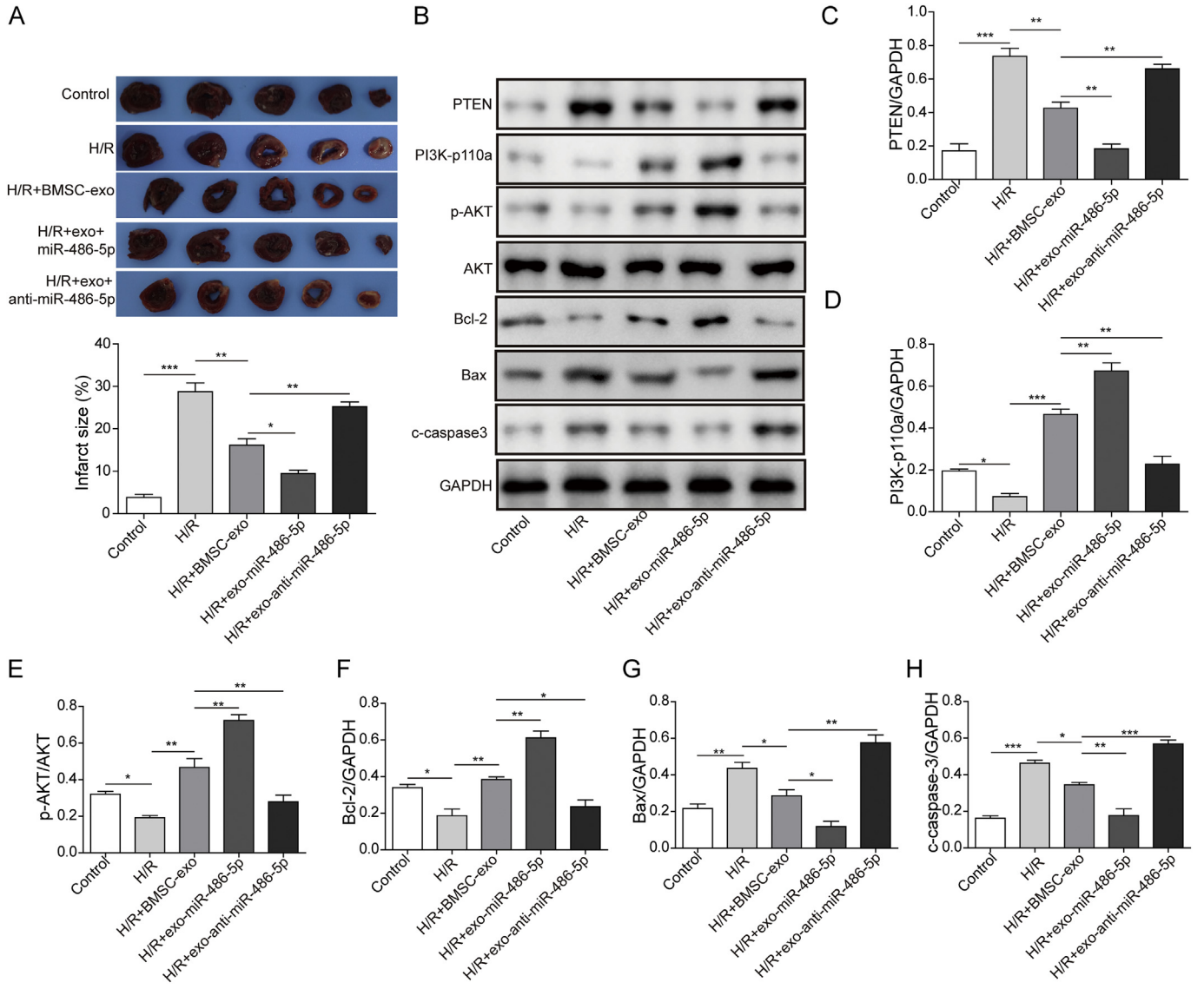

Fig. 5. MiR-486-5p from exosomes derived from bone-marrow stromal cells (BMSC-exo) decreased the myocardial injury induced by ischemia/reperfusion (I/R) via the PTEN/PI3K/AKT signaling pathway. (A) The hearts were stained with 2% (w/v) 2,3,5-triphenyltetrazolium chloride (TTC). Representative images of control rats and the myocardial infarction I/R model rats treated with exosomes are shown. Statistical analysis of infarct sizes of hearts treated with hypoxia/reoxygenation (H/R), BMSC-exo, exo-miR-486-5p or exo-anti-miR-486-5p are plotted (n = 7/group). (B) Western blot analysis of protein levels of PTEN, PI3K-p110a, p-AKT, AKT, Bcl-2, Bax and c-caspase-3 in heart tissue samples from control rats and the I/R model treated with phosphate-buffered saline (PBS) (H/R), BMSC-exo, exo-miR-486-5p or exo-anti-miR-486-5p. Glyceraldehyde 3-phosphate dehydrogenase (GAPDH) was used as internal control. (C–H) Statistical analysis of western blot results of Fig. 5B (n = 7). Data were presented as mean ± SD; $*p < 0.05$, $**p < 0.01$, $***p < 0.001$.

process of MIRI via different mechanisms, especially for exosomes derived from MSCs [17,34,35]. In this study we found that BMSC-exo significantly protects cardiomyocytes from apoptosis and MIRI. Moreover, miR-486-5p from BMSC-exo inhibited PTEN expression in cardiomyocytes, activated the PI3K/Akt signaling pathway, subsequently inhibiting cardiomyocyte apoptosis and ischemic injury to the myocardium.

BMSC-exo has been reported to have a protective effect in several diseases, including acute tubular injury [36], *Escherichia coli* endotoxin-induced acute lung injury [37], and hypoxia-induced pulmonary hypertension [38]. In the current study we demonstrated that BMSC-exo induced the proliferation of rat cardiomyocytes, which is consistent with the findings of a previous study that BMSC-exo significantly promoted the survival rate, enhanced capillary density, inhibited cardiac fibrosis, and restored long-term cardiac function [20]. Conventional treatments for ischemic heart disease—including medicinal treatment and surgery—are based on restoring blood reperfusion and inevitably result in MIRI. The newly introduced stem-cell therapy for ischemic heart disease is also facing major obstacles to long-term stem-cell and graft survival [39]. As a novel potential therapy for ischemic heart disease, BMSC-exo showed advantages in suppressing cell apoptosis, protecting cardiomyocytes from irreversible MIRI, and evading the rejection and instability of exogenous stem cells.

To further explore the mechanism by which BMSC-exo protects cardiomyocytes from ischemic injury, we investigated the involvement of miRNAs in this process. MiRNAs are generally carried by exosomes and can be released into recipient cells as key regulators. It has been reported that exosomal transferred miRNAs play important roles in the protective effect of exosomes from various sources on cardiac injury. Xiao et al. found that mouse MSCs reduced the autophagic flux in infarcted hearts via miR-125b [40]. Wang et al. reported that iPS-exo inhibited myocardial apoptosis, and the inhibition could be related to the transfer of miR-21 and miR-210 from exosomes to cardiomyocytes [19]. In the current study, we focused on miR-486-5p, the third-ranking

abundant miRNA in BMSC-exo [25], and found that the expression level of miR-486-5p in BMSC-exo was positively correlated with the protective effect of BMSC-exo on both H/R injury to cardiomyocytes and I/R injury to myocardium, suggested that BMSC-exo inhibit the apoptosis of cardiomyocytes under hypoxic conditions by releasing miR-486-5p. The anti-apoptosis activity of miR-486-5p is also supported by previous studies; miR-486-5p from exosomes derived from human endothelial colony-forming cells suppressed cell apoptosis in FVB mice with kidney ischemia/reperfusion injury [26]. MiR-486 was also reported to regulate p53-related DNA damage and the expression of cleaved caspase-3 [41,42]. Furthermore, miR-486 was shown to regulate cardiomyocyte apoptosis via a p53-mediated BCL-2-associated mitochondrial apoptotic pathway [27].

MiR-486 has been proved to be involved in the apoptosis process modulated by PTEN, PIM-1 and other effectors [43,44]. In addition, PTEN has been reported as a target for miR-486-5p [26]. The suppression of PTEN expression, which protects cardiomyocytes from apoptosis, can be induced by H/R or I/R injury [45,46]. However, PTEN targeting activity of miR-486-5p in cardiomyocytes, especially in H9C2 cells, remains unclear. In this study we evaluated the involvement of PTEN in the protective process of BMSC-exo at the level of both RNA and protein. Using a luciferase reporter assay, we demonstrated the capability of miR-486-5p from BMSC-exo to recognize the 3′-UTR of PTEN and to inhibit PTEN expression. Meanwhile, compared with BMSC-exo, treatment of *exo*-anti-miR-486-5p showed an inverse effect on PTEN level. Thus, it is suggested that miR-486-5p inhibited PTEN by sequence-specific target recognition, then suppressed the apoptosis of cardiomyocyte subsequently. BMSC-exo released miR-486-5p, which then protected the myocardium from ischemic injury by targeting PTEN and subsequently activating the PI3K/AKT pathway. Beyond that, we need to consider that PTEN is not the only direct target of miR-486-5p *in vivo*. In a study of chronic kidney disease, FOXO1 has been implicated in miR-486/PTEN/Akt signaling as the target of miR-486-5p [47]. In skeletal muscle, miR-486-5p benefited the dystrophic skeletal muscle via targeting DOCK3 and subsequently inducing phosphorylated AKT level [48]. Thus, future studies should consider more potential direct targets for miR-486-5p and other miRNAs in the overall protective effect of BMSC-exo on cardiomyocytes.

In the current study we also demonstrated that miR-486-5p from BMSC-exo inhibited PTEN and activated the PI3K/AKT signaling pathway both *in vitro* and *in vivo*, and we further investigated the significant inhibitory effect on MIRI. PI3K/AKT, an extensively studied pathway, regulates the signaling of multiple biological processes such as metabolism, apoptosis, cell proliferation and cell growth [33]. In addition, PI3K/Akt was reported to inhibit the apoptosis of cardiomyocytes directly/indirectly [49,50]. PTEN has been reported to regulate cell survival through the PI3K/Akt signaling pathway [51]. The activation of Akt phosphorylation and the PI3K/Akt pathway also appeared to be a downstream event related to PTEN inhibition [48].

To summarize: in the current study we found that BMSC-exo inhibited cardiomyocyte apoptosis induced by H/R, protecting cardiomyocytes from ischemic injury both *in vitro* and *in vivo*. In further exploration of the mechanism, we found that BMSC-exo down-regulated the PTEN level, activated the PI3K/AKT signaling pathway, and then protected injured cardiomyocytes via miR-486-5p. The exploration of the active component and functional mechanism of BMSC-exo is of much significance to developing a new biotherapy of myocardial ischemia based on exosomes. This study preliminarily clarified the mechanism of BMSC-exo protecting ischemic myocardium, offering a new approach to alleviating myocardium ischemic injury.

References

[1] G. Lippi, M. Franchini, G. Cervellin, Diagnosis and management of ischemic heart disease, Semin. Thromb. Hemost. 39 (2) (2013) 202–213.

[2] A. Frank, et al., Myocardial ischemia reperfusion injury: from basic science to clinical bedside, Semin. Cardiothorac. Vasc. Anesth. 16 (3) (2012) 123–132.

[3] K.R. Bainey, P.W. Armstrong, Clinical perspectives on reperfusion injury in acute myocardial infarction, Am. Heart J. 167 (5) (2014) 637–645.

[4] R. Ramaraj, Myocardial reperfusion injury, N. Engl. J. Med. 357 (23) (2007) 2408 (author reply 2409-10).

[5] Z.Q. Zhao, J. Vinten-Johansen, Myocardial apoptosis and ischemic preconditioning, Cardiovasc. Res. 55 (3) (2002) 438–455.

[6] J.W. Hoffman Jr.et al., Myocardial reperfusion injury: etiology, mechanisms, and therapies, J Extra Corpor Technol 36 (4) (2004) 391–411.

[7] S. Chakrabarti, A.N. Hoque, M. Karmazyn, A rapid ischemia-induced apoptosis in isolated rat hearts and its attenuation by the sodium-hydrogen exchange inhibitor HOE 642 (cariporide), J. Mol. Cell. Cardiol. 29 (11) (1997) 3169–3174.

[8] G. Raposo, W. Stoorvogel, Extracellular vesicles: exosomes, microvesicles, and friends, J. Cell Biol. 200 (4) (2013) 373–383.

[9] C. Thery, Exosomes: secreted vesicles and intercellular communications, F1000 Biol. Rep. 3 (2011) 15.

[10] T. Tian, et al., Visualizing of the cellular uptake and intracellular trafficking of exosomes by live-cell microscopy, J. Cell. Biochem. 111 (2) (2010) 488–496.

[11] A. Waldenstrom, et al., Cardiomyocyte microvesicles contain DNA/RNA and convey biological messages to target cells, PLoS One 7 (4) (2012) e34653.

[12] N. Chaput, C. Thery, Exosomes: immune properties and potential clinical implementations, Semin. Immunopathol. 33 (5) (2011) 419–440.

[13] C.W. Kim, et al., Extracellular membrane vesicles from tumor cells promote angiogenesis via sphingomyelin, Cancer Res. 62 (21) (2002) 6312–6317.

[14] M.C. Deregibus, et al., Endothelial progenitor cell derived microvesicles activate an angiogenic program in endothelial cells by a horizontal transfer of mRNA, Blood 110 (7) (2007) 2440–2448.

[15] B.S. Hong, et al., Colorectal cancer cell-derived microvesicles are enriched in cell cycle-related mRNAs that promote proliferation of endothelial cells, BMC Genomics 10 (2009) 556.

[16] S. Bian, et al., Extracellular vesicles derived from human bone marrow mesenchymal stem cells promote angiogenesis in a rat myocardial infarction model, J. Mol. Med. 92 (4) (2014) 387–397.

[17] R.C. Lai, et al., Exosome secreted by MSC reduces myocardial ischemia/reperfusion injury, Stem Cell Res. 4 (3) (2010) 214–222.

[18] L. Chen, et al., Cardiac progenitor-derived exosomes protect ischemic myocardium from acute ischemia/reperfusion injury, Biochem. Biophys. Res. Commun. 431 (3) (2013) 566–571.

[19] Y. Wang, et al., Exosomes/microvesicles from induced pluripotent stem cells deliver cardioprotective miRNAs and prevent cardiomyocyte apoptosis in the ischemic myocardium, Int. J. Cardiol. 192 (2015) 61–69.

[20] Z. Zhang, et al., Pretreatment of cardiac stem cells with exosomes derived from mesenchymal stem cells enhances myocardial repair, J. Am. Heart Assoc. 5 (1) (2016).

[21] D.P. Bartel, MicroRNAs: genomics, biogenesis, mechanism, and function, Cell 116 (2) (2004) 281–297.

[22] A.G. Ibrahim, K. Cheng, E. Marban, Exosomes as critical agents of cardiac regeneration triggered by cell therapy, Stem Cell Rep. 2 (5) (2014) 606–619.

[23] Y. Feng, et al., Ischemic preconditioning potentiates the protective effect of stem cells through secretion of exosomes by targeting Mecp2 via miR-22, PLoS One 9 (2) (2014) e88685.

[24] Z. Wen, et al., Bone marrow mesenchymal stem cells for post-myocardial infarction cardiac repair: microRNAs as novel regulators, J. Cell. Mol. Med. 16 (4) (2012) 657–671.

[25] S.R. Baglio, et al., Human bone marrow- and adipose-mesenchymal stem cells secrete exosomes enriched in distinctive miRNA and tRNA species, Stem Cell Res. Ther. 6 (2015) 127.

[26] J.L. Vinas, et al., Transfer of microRNA-486-5p from human endothelial colony forming cell-derived exosomes reduces ischemic kidney injury, Kidney Int. 90 (6) (2016) 1238–1250.

[27] Y. Sun, et al., MiR-486 regulates cardiomyocyte apoptosis by p53-mediated BCL-2 associated mitochondrial apoptotic pathway, BMC Cardiovasc. Disord. 17 (1) (2017) 119.

[28] X. Zhang, et al., MicroRNA-486 alleviates hypoxia-induced damage in H9c2 cells by targeting NDRG2 to inactivate JNK/C-Jun and NF-kappaB signaling pathways, Cell. Physiol. Biochem. 48 (6) (2018) 2483–2492.

[29] A. Carnero, et al., The PTEN/PI3K/AKT signalling pathway in cancer, therapeutic implications, Curr. Cancer Drug Targets 8 (3) (2008) 187–198.

[30] J. Kajstura, et al., Apoptotic and necrotic myocyte cell deaths are independent contributing variables of infarct size in rats, Lab. Investig. 74 (1) (1996) 86–107.

[31] W. Cheng, et al., Programmed myocyte cell death affects the viable myocardium after infarction in rats, Exp. Cell Res. 226 (2) (1996) 316–327.

[32] A. Saraste, et al., Apoptosis in human acute myocardial infarction, Circulation 95 (2) (1997) 320–323.

[33] M. Tanaka, et al., Hypoxia induces apoptosis with enhanced expression of Fas antigen messenger RNA in cultured neonatal rat cardiomyocytes, Circ. Res. 75 (3) (1994) 426–433.

[34] F. Arslan, et al., Mesenchymal stem cell-derived exosomes increase ATP levels, decrease oxidative stress and activate PI3K/Akt pathway to enhance myocardial viability and prevent adverse remodeling after myocardial ischemia/reperfusion injury, Stem Cell Res. 10 (3) (2013) 301–312.

[35] R.C. Lai, et al., Proteolytic potential of the MSC exosome proteome: implications for an exosome-mediated delivery of therapeutic proteasome, Int. J. Proteomics 2012 (2012) 971907.

[36] S. Bruno, et al., Mesenchymal stem cell-derived microvesicles protect against acute tubular injury, J. Am. Soc. Nephrol. 20 (5) (2009) 1053–1067.

[37] Y.G. Zhu, et al., Human mesenchymal stem cell microvesicles for treatment of Escherichia coli endotoxin-induced acute lung injury in mice, Stem Cells 32 (1) (2014) 116–125.
[38] C. Lee, et al., Exosomes mediate the cytoprotective action of mesenchymal stromal cells on hypoxia-induced pulmonary hypertension, Circulation 126 (22) (2012) 2601–2611.
[39] P.K. Nguyen, et al., Imaging: guiding the clinical translation of cardiac stem cell therapy, Circ. Res. 109 (8) (2011) 962–979.
[40] C. Xiao, et al., Transplanted mesenchymal stem cells reduce autophagic flux in infarcted hearts via the exosomal transfer of mir-125b, Circ. Res. (2018).
[41] K.M. Keller, S.E. Howlett, Sex differences in the biology and pathology of the aging heart, Can. J. Cardiol. 32 (9) (2016) 1065–1073.
[42] S.M. Dunlay, V.L. Roger, Gender differences in the pathophysiology, clinical presentation, and outcomes of ischemic heart failure, Curr. Heart Fail. Rep. 9 (4) (2012) 267–276.
[43] M. Narasimhan, N.S. Rajasekaran, Exercise, Nrf2 and antioxidant signaling in cardiac aging, Front. Physiol. 7 (2016) 241.
[44] G. Takemura, et al., Cardiomyocyte apoptosis in the failing heart—a critical review from definition and classification of cell death, Int. J. Cardiol. 167 (6) (2013) 2373–2386.
[45] Q. Yang, K. Yang, A.Y. Li, Trimetazidine protects against hypoxia-reperfusion-induced cardiomyocyte apoptosis by increasing microRNA-21 expression, Int. J. Clin. Exp. Pathol. 8 (4) (2015) 3735–3741.
[46] Z.P. Ke, et al., MicroRNA-93 inhibits ischemia-reperfusion induced cardiomyocyte apoptosis by targeting PTEN, Oncotarget 7 (20) (2016) 28796–28805.
[47] J. Xu, et al., Transcription factor FoxO1, the dominant mediator of muscle wasting in chronic kidney disease, is inhibited by microRNA-486, Kidney Int. 82 (4) (2012) 401–411.
[48] M.S. Alexander, et al., MicroRNA-486-dependent modulation of DOCK3/PTEN/AKT signaling pathways improves muscular dystrophy-associated symptoms, J. Clin. Invest. 124 (6) (2014) 2651–2667.
[49] J. Sakamaki, et al., Arginine methylation of BCL-2 antagonist of cell death (BAD) counteracts its phosphorylation and inactivation by Akt, Proc. Natl. Acad. Sci. U. S. A. 108 (15) (2011) 6085–6090.
[50] D.Y. Lu, et al., SDF-1alpha up-regulates interleukin-6 through CXCR4, PI3K/Akt, ERK, and NF-kappaB-dependent pathway in microglia, Eur. J. Pharmacol. 613 (1–3) (2009) 146–154.
[51] L.C. Cantley, B.G. Neel, New insights into tumor suppression: PTEN suppresses tumor formation by restraining the phosphoinositide 3-kinase/AKT pathway, Proc. Natl. Acad. Sci. U. S. A. 96 (8) (1999) 4240–4245.